



Research papers

Nitrous oxide processing in carbonate karst aquifers



Madison K. Flint^{a,*}, Jonathan B. Martin^a, Tatiana I. Summerall^a, Adrian Barry-Sosa^b, Brent C. Christner^b

^a Department of Geological Sciences, University of Florida, 241 Williamson Hall, Gainesville, FL 32611-2120, United States

^b Department of Microbiology & Cell Science, University of Florida, 1355 Museum Drive, Gainesville, FL 32611-0700, United States

ARTICLE INFO

Keywords:

Greenhouse gases
Nitrogen
Nitrous oxide
Karst
Groundwater
Springs

ABSTRACT

The increased environmental abundance of anthropogenic reactive nitrogen species (N_r = ammonium [NH_4^+], nitrite [NO_2^-] and nitrate [NO_3^-]) may increase atmospheric nitrous oxide (N_2O) concentrations, and thus global warming and stratospheric ozone depletion. Nitrogen cycling and N_2O production, reduction, and emissions could be amplified in carbonate karst aquifers because of their extensive global range, susceptibility to nitrogen contamination, and groundwater-surface water mixing that varies redox conditions of the aquifer. The magnitude of N_2O cycling in karst aquifers is poorly known, however, and thus we sampled thirteen springs discharging from the karstic Upper Floridan Aquifer (UFA) to evaluate N_2O cycling. The springs can be separated into three groups based on variations in subsurface residence times, differences in surface-groundwater interactions, and variable dissolved organic carbon (DOC) and dissolved oxygen (DO) concentrations. These springs are oxic to sub-oxic and have NO_3^- concentrations that range from < 0.1 to $4.2 \text{ mg N-NO}_3^-/\text{L}$ and DOC concentrations that range from < 0.1 to 50 mg C/L . Maximum spring water N_2O concentrations are $3.85 \mu\text{g N-N}_2\text{O}/\text{L}$ or ~ 12 times greater than water equilibrated with atmospheric N_2O . The highest N_2O concentrations correspond with the lowest NO_3^- concentrations. Where recharge water has residence times of a few days, partial denitrification to N_2O occurs, while complete denitrification to N_2 is more prominent in springs with longer subsurface residence times. Springs with short residence times have groundwater emission factors greater than the global average of 0.0060, reflecting N_2O production, whereas springs with residence times of months to years have groundwater emission factors less than the global average. These findings imply that N_2O cycling in karst aquifers depends on DOC and DO concentrations in recharged surface water and subsequent time available for N processing in the subsurface.

1. Introduction

Since the start of the 20th century, anthropogenic production of N_r species has increased by a factor of 10, largely from fossil fuel burning and industrial application of the Haber-Bosch process (Galloway and Cowling, 2002; Galloway et al., 2004). Since the end of the 20th century, anthropogenic fixation of atmospheric N_2 has exceeded that of natural terrestrial N_2 fixation (Galloway and Cowling, 2002). The subsequent accumulation of anthropogenic N_r has important ecological implications through eutrophication and enhancing primary productivity in aquatic systems. Additional environmental impacts result from processing of N_r in aquatic ecosystems including anoxia, which creates conditions favorable for the microbial transformation of N species such as N_2O .

N_2O is a powerful greenhouse gas with an atmospheric lifespan of approximately 121 years and a warming potential about 265 times that

of carbon dioxide (CO_2) and 10 times that of methane (CH_4) (Myhre et al., 2013). In addition to its greenhouse warming potential, N_2O has been the single most important stratospheric ozone depleting substance emitted in the 21st century (Ravishankara et al., 2009). Since pre-industrial times, global N_2O emissions have increased approximately 20% in parallel with increased N_r abundance (Galloway et al., 2008; Butterbach-Bahl et al., 2013), with emissions projected to double by 2050 (Davidson & Kanter, 2014). Nearly 40% of total N_2O emissions are anthropogenic in nature and originate from a combination of fossil fuel combustion, industrial activities, and agriculture, with the latter estimated to be the largest contributor (Jurado et al., 2018). Although N_2O is produced by abiotic reactions and microbial metabolisms, production through microbial denitrification and nitrification are the greatest contributors to global N_2O emissions (Thomson et al., 2012).

Karst aquifers have physicochemical characteristics that are ideal for

* Corresponding author.

E-mail address: mflint@ufl.edu (M.K. Flint).

<https://doi.org/10.1016/j.jhydrol.2020.125936>

N_r processing, including extensive and rapid surface water-groundwater interactions and highly heterogeneous permeability that leads to spatially variable redox conditions (Ford and Williams, 2007). Karst landscapes cover approximately 20% of Earth's ice-free land surface (Goldscheider et al., 2020), and depending on the extent of N_r processing, they could significantly effect global N_2O cycling. However, few studies to date have investigated N_2O cycling within carbonate aquifers despite their large spatial distribution and potential for N_r processing. This processing would be affected by exchange of surface water and groundwater, which controls availability of electron donors (e.g., organic carbon, reduced Fe, Mn, S; NH_4^+) and electron acceptors (e.g., NO_3^- ; O_2), aquifer redox conditions, and abiotic and/or microbial reactions.

N_2O is an intermediate of denitrification and is produced when NO_3^- is microbially respired and sequentially reduced to N_2 . N_2O production via denitrification has been reported under anoxic to oxic conditions for karstic groundwater (Albertin et al., 2012; Heffernan et al., 2012; Jahangir et al., 2013; Henson et al., 2019). Nitrification is an obligately aerobic process in which N_2O is produced during NH_4^+ oxidation to NO_2^- as a by-product during abiotic decomposition of the intermediate species hydroxylamine (NH_2OH) (Thomson et al., 2012). Nitrification has been hypothesized to be active in karstic groundwater and contribute to elevated N_2O concentrations (Ueda et al., 1993; Mühlherr and Hiscock,

1998; Hiscock et al., 2003; Jurado et al., 2018), but direct evidence has been lacking.

In this study we addressed three primary questions: 1) could karstic springs be an atmospheric source of N_2O ; 2) do N_2O concentrations change with space and time across a karst landscape; and 3) how much N_r (primarily NO_3^-) is reduced to N_2O ? The study area is the karstic Upper Floridan Aquifer (UFA) in north-central Florida, USA (Fig. 1), where previous studies provide much information on the timing of surface water and groundwater exchange and subsurface residence times of water discharging from multiple springs. Analyses of the chemical compositions of the spring water reveal systematic relationships between the residence times, organic carbon contents, and N_2O concentrations that point toward potential controls on N_2O production and consumption.

2. Site descriptions: geological and hydrological settings

The study area is within the Suwannee River watershed and is underlain by the carbonate Eocene to Oligocene carbonate strata (Fig. 1A–B). These strata include the Suwannee Limestone (10–30 m thickness), Ocala Limestone (20–80 m thickness), and Avon Park Formation (Sutton et al., 2015). Within the watershed, the UFA is unconfined in the lower reaches and confined in the upper reaches by the Miocene Hawthorn

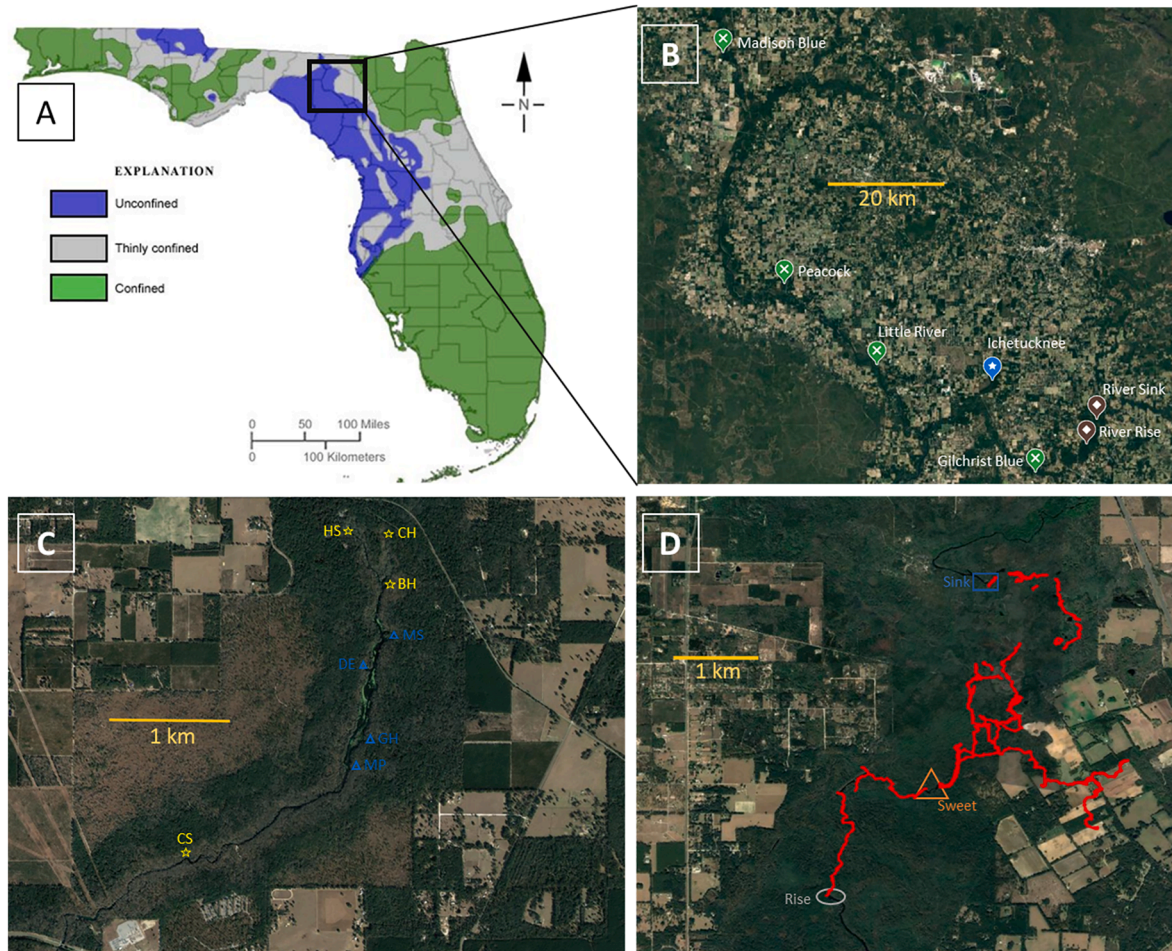


Fig. 1. A. Map of north-central Florida highlighting the study region and indicating the areas of confined and unconfined UFA as represented by the Cody Escarpment [modified image from Walsh, 2001]; B. Google Earth images of study sites showing the location of the Ichetucknee springs group (blue point), the reversing springs group (green points), and the Santa Fe Sink-Rise system (brown points). All springs discharge from the unconfined portion of the UFA; C. Within the Ichetucknee system are 8 major named springs including group 1a springs (yellow stars): Cedar Head (CH), Head Springs (HS), Blue Hole (BH), Coffee Springs (CS) and group 1b springs (blue triangles): Mission Springs (MS), Mill Pond (MP), Devil's Eye (DE), Grassy Hole (GH); D. Within the Santa Fe system are the River Sink, Sweetwater, and River Rise. Mapped conduits from River Sink, to Sweetwater, to River Rise are outlined in red [Suwannee River Water Management District, <https://acwi.gov/monitoring/conference/2014/2ConcurrentSessions/G2/G2Shortelle.pdf>, accessed October 22nd, 2020].

Group. The boundary between the confined and unconfined portion of the UFA, called the Cody Escarpment (Puri and Vernon, 1964), is the erosional edge of the Hawthorn Group and is the site of extensive surface water-groundwater exchange (Fig. 1A). All streams flowing across the escarpment either sink completely into the subsurface or become losing streams.

The UFA is characterized by intergranular primary porosity of about 20% and can be classified as an eogenetic karst aquifer (Vacher and Mylroie, 2002). This primary porosity, with an average matrix permeability of 10^{-13} m² for the Ocala limestone, can provide storage for recharged surface water during flooding events (Florea and Vacher, 2006). At base flow, the matrix porosity may provide 25–50% of groundwater flow to the numerous springs that discharge from water-filled caves in the UFA downstream of the Cody Escarpment (Rosenau et al., 1977; Scott et al., 2002; Ritorto et al., 2009; Yang et al., 2019). Regional groundwater flow across the watershed is predominately toward the southwest and includes both slow matrix and fast conduit/fracture flow. We focus on 13 springs that can be separated into three groups with variable rates of surface water-groundwater interactions, chemical compositions, and groundwater residence times.

One group of springs, the Ichetucknee springs group (Fig. 1C), includes eight named springs and numerous unnamed smaller springs that discharge <1 to 5.6 m³/sec to the Ichetucknee River (Scott et al., 2002). This group has the lowest DOC concentrations among the studied spring groups (Table 1). The Ichetucknee springs group can be divided into two sub-groups based on their chemical compositions (Martin & Gordon, 2000) and apparent ages (Martin et al., 2016). Group 1a springs (Head Spring, Blue Hole, Cedar Head, and Coffee Springs) have higher dissolved oxygen (DO) concentrations and more variable temperatures (ΔT 0.3–0.5 °C) than group 1b springs (Mission Springs, Devil's Eye, Mill Pond, and Grassy Hole). The mean apparent ages based on CFC-12 concentrations of group 1a springs (35.08 ± 0.20 years) is younger than group 1b springs (40.47 ± 0.28 years; Table 2). These characteristics suggest that group 1a springs have shorter and shallower flow paths than group 1b springs (Martin & Gordon, 2000).

The second group of springs are referred to as “reversing springs” (Peacock, Madison Blue, Little River, and Gilchrist Blue) because river water with DOC and DO concentrations greater than groundwater values (Table 1) periodically intrudes through the spring vents during high flow conditions (Gulley et al., 2011; Brown et al., 2014, 2019). These reversals occur once or twice a year and flood water may reside in the aquifer for days to months before draining back to the surface as the floods recede. Of this group, mean apparent age has been measured only for Little River Spring. The average apparent age, which is based on CFC-12 concentrations, is ~21 years (Katz et al., 2001; Heffernan et al., 2012; Table 2). This apparent age is likely much longer than water that discharges immediately following a reversal, when residence times may be days to months (e.g., Gulley et al., 2011; Brown et al., 2014). As DOC and DO are biogeochemically processed in the aquifer, groundwater redox state shifts as reflected by variable Fe and Mn concentrations in water discharging from Madison Blue Spring following reversals (Brown et al., 2019).

The third group of springs are part of a Sink-Rise system that occurs where the Santa Fe River crosses the Cody Escarpment (Fig. 1D). Except during flooding, all river water is captured by a sinkhole called River Sink. The river briefly resurges at several karst windows, most prominently at Sweetwater Lake, before discharging permanently at River Rise Spring approximately 7 km downstream from River Sink (Scott et al., 2002). Water recharged at River Sink requires from 6 to 185 h to flow to River Rise depending on river stage (Fig. S1) and River Rise discharge is commonly greater than discharge into River Sink. The downstream increase in flow reflects water gained from matrix porosity to the conduits when the groundwater hydraulic head exceeds that of the conduits, which should increase average residence times and specific conductivity (SpC) of the discharging water at River Rise (Martin and Dean, 1999; Moore et al., 2009). River Sink discharge can exceed River Rise

discharge during high flow events when the conduit hydraulic head is greater than that of the groundwater. During these conditions, water is assumed to be lost from conduits to matrix porosity (Martin and Dean, 1999; Bailly-Comte et al., 2010, 2011).

3. Methods

Water was pumped directly from spring vents using a Geotech peristaltic pump and tubing that extended to the shore. At the Santa Fe Sink-Rise system, water was pumped through an overflow cup containing sondes connected to a YSI ProPlus meter that was calibrated daily. At all other locations, the sondes were deployed directly in the path of discharge above spring vents. Measured parameters were dissolved oxygen concentrations (DO% saturation and mg/L), specific conductivity ($\mu\text{S}/\text{cm}$), and temperature (°C). Parameters were monitored until values stabilized, typically within a few minutes, after which the physicochemical parameters were recorded, and sampling commenced.

Samples to be measured for total DOC, total dissolved nitrogen (TDN = inorganic-N + organic-N), NO_3^- , and SO_4^{2-} concentrations were filtered through 0.45- μm trace metal grade canister filters. The DOC and TDN samples were preserved with concentrated HCl and nitrate samples were frozen until analysis. N_2O samples were collected via the headspace extraction method (Pain et al., 2019 e.g., Repo et al., 2007) in a 650 mL vessel with 60 mL of sample water displaced with ultra-high purity grade helium (UHP; 99.999% purity) or N_2 (UHP) and shaken to equilibration for 3 min. The 60 mL of headspace gas was immediately transferred to pre-evacuated 75 mL glass vials and analyzed within 1 week of collection.

The N_2O concentrations were measured at the University of Florida with an Agilent Gas Chromatograph (7820-A) equipped with a $\mu\text{-ECD}$ (electron capture detector - ^{63}Ni source, 350 °C, makeup gas 5% CH_4/Argon mixture) and an Agilent J&W GS-CARBONPLOT column (30 m length, 0.320 mm diameter widebore, 3.00 μm film) regulated at a temperature of 30 °C and UHP N_2 as the carrier gas. Calibration standards were prepared by diluting a 0.9700 ppm N_2O standard in a He or N_2 matrix to 0%, 25%, 50%, 75%, 100% N_2O . Dilutions were made fresh before each analysis by injecting gases directly into pre-evacuated 75 mL glass vials. Gas concentrations in the headspace samples were converted to dissolved concentrations according to Weiss et al., 1980 and based on the temperature and salinity of the water. All N_2O samples were collected in triplicate to assess the relative error of the head-space extraction collection method, which generated a relative standard deviation of <0.2 $\mu\text{g N-N}_2\text{O}/\text{L}$. The saturation of N_2O was calculated as a percentage relative to atmospheric equilibration with water using the method reported by Cooper et al. (2017). Atmospheric concentration was referenced to the 2019 global average of 332 ppb [https://www.esrl.noaa.gov/gmd/ccgg/trends_n2o/ - accessed January 2019], or approximately 0.3 $\mu\text{g N-N}_2\text{O}/\text{L}$ at 21.5 °C and 0.1 ppt salinity. This global average is similar to the average atmospheric N_2O concentrations measured in our field area of 330 ppb (range 304–356 ppb, $n = 17$) during the course of this study.

In-situ NO_3^- concentrations in clear spring waters of the Ichetucknee and reversing springs group were measured with a Submersible Ultraviolet Nitrate Analyzer (SUNA), which measures NO_3^- concentrations based on absorbance at wavelengths from 217 to 240 nm. At the Sink-Rise system, elevated DOC interferes with the SUNA and these samples were measured with an automated Dionex ICS-2100 Ion Chromatograph at the University of Florida. Clear water spring samples of the Ichetucknee and reversing springs groups measured for NO_3^- concentrations with both the SUNA and ion chromatography were similar (± 0.05 mg N- NO_3^-/L difference). The ion chromatograph was also used to measure SO_4^{2-} concentrations, with an error on replicates of <5% and a detection limit of 0.01 mg S- $\text{SO}_4^{2-}/\text{L}$ and 0.01 mg N- NO_3^-/L . DOC and TDN concentrations were analyzed on a Shimadzu TOC-VCSN total element analyzer at the University of Florida and the coefficient of

Table 1
Summary of geochemical parameters, solute concentrations, and emission factors within spring and surface waters of the karstic UFA during a ~ 2-year period (7.28.2018 – 9.5.2020).

Spring type	Ichetucknee Group 1b				Ichetucknee Group 1a				Reversing Springs Group				Santa Fe System			
Location name	Mill Pond	Mission Springs	Devil's Eye	Grassy Hole	Coffee Springs	Blue Hole	Head Spring	Cedar Head	Gilchrist Blue vents	Madison Blue	Little River	Peacock Springs	River Sink	Sweet water	River Rise	
Sample dates	10.6.18	9.14.18	8.10.18 - 4.17.19	9.14.18	8.10.18 - 10.27.18	8.4.18 - 6.23.19	8.4.18 - 1.25.20	11.11.18 - 1.25.20	7.30.18 - 12.6.18	10.17.18 - 9.5.20	4.8.19	10.17.18 - 9.5.20	8.26.18 - 8.9.20	8.26.18 - 7.21.20	7.28.18 - 8.9.20	
Sample points (n)	n=1	n=1	n=4	n=1	n=4	n=4	n=7	n=2	n=3	n=3	n=1	n=4	n=25	n=13	n=27	
SpC (µS/cm)	378.6	318.9	337.6 - 341.9	360.8	292.0 - 302.9	252.9 - 323.9	316.6 - 349.4	316.6 - 317.9	356.8 - 400.0	292.1 - 299.9	406.5	411.6 - 441.1	64.4 - 359.7	70.9 - 476.2	69.3 - 526.0	
Temp (°C)	21.7	21.7	21.6 - 21.8	21.8	21.7	21.6 - 21.9	21.6 - 21.9	21.4 - 21.5	22.4 - 22.5	20.9 - 21.0	21.4	21.5 - 21.7	12.9 - 26.5	14.5 - 25.4	14.1 - 25.5	
DO (mg/L)	0.31	0.28	0.11 - 1.15	0.46	2.45 - 3.20	1.81 - 2.16	3.65 - 4.13	2.51 - 2.61	4.72	1.38 - 1.83	2.03	1.30 - 2.68	2.61 - 9.30	0.96 - 7.83	0.65 - 7.16	
DOC (mg C/L)	0.33	0.71	0.30 - 0.51 (n=2)	0.34	0.08 - 0.22 (n=2)	0.19 - 1.3 (n=2)	0.17 - 0.29 (n=4)	0.83 (n=1)	0.46 - 0.49 (n=2)	0.26 - 0.54 (n=2)	4.6	0.38 - 0.69 (n=3)	3.9 - 58.8 (n=23)	2.5 - 38.4 (n=11)	2.4 - 50.2 (n=24)	
SO ₄ ²⁻ (mg S/L)	9.37	2.64	4.61 - 5.22 (n=2)	6.97	3.31 (n=2)	1.70 (n=1)	2.83 - 3.17 (n=4)	2.25 (n=1)	—	4.13 - 4.51 (n=2)	—	7.56 - 7.86 (n=3)	0.71 - 32.4 (n=23)	1.30 - 29.5 (n=11)	0.95 - 31.2 (n=24)	
NO ₃ ⁻ (mg N/L)	0.66	0.70	0.74 (n=1)	0.57	0.63 (n=1)	0.79 (n=2)	0.77 - 0.82 (n=3)	0.90 (n=2)	2.3 - 2.5 (n=2)	2.0 - 2.2	1.9	3.4 - 4.2	< 0.01 - 0.31 (n=23)	0.01 - 0.53 (n=11)	< 0.01 - 0.53 (n=24)	
N ₂ O (µg N/L)	0.46	0.53	0.41 - 1.01	0.57	0.68 - 0.78	1.24 - 1.36	1.37 - 1.57	1.68 - 1.72	1.55 - 1.66	1.56 - 1.86	2.76	2.27 - 2.90	0.25 - 5.35	0.34 - 3.10	0.22 - 3.85	
TDN (mg N/L)	0.50	0.68	0.68 - 0.72 (n=2)	0.61	0.44 - 0.45 (n=2)	0.79 - 0.93 (n=2)	0.80 - 0.82 (n=4)	0.85 (n=1)	2.7 - 2.8 (n=2)	2.0 - 2.4 (n=2)	1.9	3.1 - 3.8 (n=3)	0.23 - 1.3 (n=23)	0.35 - 1.1 (n=11)	0.34 - 1.2 (n=24)	
EF _{5g} (N ₂ O / NO ₃ ⁻)	0.0007	0.0008	0.0012	0.0010	0.0011	0.0017	0.0017 - 0.0018	0.0019	0.0007	0.0007 - 0.0009	0.0015	0.0007	0.0035 - 0.0627 (EF _{5r} - base flow, n=17)	0.0031 - 0.0122 (base flow, n=8)	0.0032 - 0.0177 (base flow, n=18)	
EF _{5g} (N ₂ O / TDN)	0.0009	0.0008	0.0010 - 0.0012	0.0009	0.0016	0.0013 - 0.0017	0.0017 - 0.0018	0.0019	0.0006	0.0007 - 0.0009	0.0015	0.0006 - 0.0009	0.0009 - 0.0131 (EF _{5r} - base flow, n=17)	0.0009 - 0.0080 (base flow, n=8)	0.0007 - 0.0113 (base flow, n=18)	

Table 2
Summary of geochemistry within the Ichetucknee system*.

Spring Group	Vent	Apparent Age (years) ^a	DO (mg/L)	N ₂ O (µg N/L)	Excess N ₂ (mg N/L) ^{b, c}	NO ₃ ⁻ (mg N/L)	δ ¹⁵ N-NO ₃ ⁻ (‰) ^{b, c, d}	δ ¹⁸ O-NO ₃ ⁻ (‰) ^{b, c, d}
Reversing Springs Group	Little River	21 ^{b, f}	1.43	2.76	0.95 ^b	1.86	6.9 ^b	7.9 ^c
							5.7 – 11.0 ^e	7.8 – 11.1 ^e
Ichetucknee sub-group 1a	Cedar Head	36	2.56	1.7	0.97 ^c	0.9	3.3 ^c	4.8 ^c
							3.6 ^d	7.2 ^d
	Head Spring	34	3.96	1.42	0.27 ^b	0.8	2.7 ^b	6.8 ^b
							3.4 ^c	4.6 ^c
Blue Hole	36	2.09	1.32	0.52 ^b	0.79	3.5 ^d	7.0 ^d	
						3.5 ^b	7.7 ^b	
Ichetucknee sub-group 1b	Coffee Springs	36	2.52	0.7	—	0.63	—	—
							Devil's Eye	40
	Mission Springs	39	0.28	0.53	0.55 ^b	0.7		
							Mill Pond	42
	Grassy Hole	40	0.46	0.57	—	0.56		
							7.5 ^d	11.7 ^d
							13.7 ^b	18.6 ^b
							6.3 ^c	8.3 ^c
							12.5 ^d	13.8 ^d

*Data collected in 2018 (this paper), compiled with data from [Martin et al. \(2016\)](#); **B:** [Heffernan et al. 2012 \(2010\)](#); **C:** [Katz et al., 2009 \(2007\)](#); **D:** [Cohen et al. 2012 \(2008–2009\)](#); **E:** [Albertin et al., 2012 \(2006–2008\)](#); and **F:** [Katz et al., 2001](#) discussing N dynamics within the basin (DO, N₂O and NO₃⁻ from this study are reported as median values). Years in parentheses are sampling times.

variation was less than 2% between sample replicates. A Student's *t*-test assuming unequal variances was conducted for the different physical and geochemical characteristics of the Ichetucknee spring sub-groups (groups 1a and 1b). Statistical significance of samples was based on *P*-values < 0.05 ([Table 1](#)).

To evaluate potential reduction of NO₃⁻ to N₂O, groundwater emission factors were calculated as the ratio of N₂O (mg N-N₂O/L) to NO₃⁻ (mg N-NO₃⁻/L) concentrations in discharging spring waters according to:

$$EF_{NO_3^-} = \frac{N_2O}{NO_3^-} \quad (1)$$

(e.g. IPCC, [Hergoualc'h et al., 2019](#)). Reduction of NO₃⁻ and oxidation of NH₄⁺ may also contribute to N₂O production; however, we lack comprehensive measurements of these solute concentrations. Within spring waters discharging from the unconfined portion of the UFA, N_r primarily exists as NO₃⁻ while NH₄⁺ concentrations have been reported to be ≤ 0.02 mg N/L ([Katz et al., 2009](#)) and concentrations of NO₂⁻ are expected to be equally low or lower. We estimate contributions of NH₄⁺ and NO₂⁻ to calculated emission factors based on the TDN (mg N/L) concentrations according to:

$$EF_{TDN} = \frac{N_2O}{TDN} \quad (2)$$

Other redox sensitive solutes, including ferrous iron (Fe²⁺) and hydrogen sulfide (HS⁻), were measured in the field as initial samples were collected from all springs using a field spectrophotometer (Hach DR 890 portable colorimeter). Concentrations were below instrumental detection limits (0.01 mg/L for both Fe²⁺ and SH⁻), suggesting these solutes provide little control on redox conditions of spring waters.

4. Results

4.1. Ichetucknee springs group

Chemical compositions of the two Ichetucknee spring sub-groups are similar to previous observations ([Martin and Gordon, 2000](#); [Martin et al., 2016](#)). Median SpC values and TDN concentrations are significantly lower in group 1a springs than group 1b ([Table 1](#)). In contrast, median DO, NO₃⁻, and SO₄²⁻ concentrations are significantly higher in

group 1a spring waters than group 1b springs (*p* < 0.05) ([Table 1](#)). TDN concentrations do not significantly exceed NO₃⁻ concentrations (~0.05 mg N/L; [Table 1](#)), suggesting NO₃⁻ is the dominate N_r species present in Ichetucknee spring waters. Group 1b springs have significantly lower N₂O concentrations, with a range from 0.41 to 1.01 µg N-N₂O/L (median = 0.57), than group 1a springs which range from 0.68 to 1.72 µg N-N₂O/L (median = 1.37) (*p* < 0.05). These concentrations reflect oversaturation relative to the atmosphere ranging from 132% at Devil's Eye (group 1b) to 558% at Cedar Head Spring (group 1a) ([Fig. 2](#)). The DO and NO₃⁻ concentrations correlate positively with N₂O concentrations while SO₄²⁻ concentrations are inversely correlated and DOC concentrations show no correlation ([Fig. 3](#)). Median values for EF_{NO3}⁻ range from 0.0007 to 0.0019 (Eq. (1)) and group 1b springs have lower median values (0.0009) than group 1a springs (0.0018). Median values of EF_{TDN} (Eq. (2)) are similar to the EF_{NO3}⁻ value, ranging from 0.0009 and 0.0017 for sub-groups 1b and 1a, respectively ([Table 1](#)).

4.2. Reversing springs group

The reversing springs group has median SpC values and DO concentrations of 400 µS/cm and 1.83 mg/L, respectively. This spring group has higher NO₃⁻ concentrations than the other two spring groups, with a range from 1.9 mg N/L at Little River Spring to 4.2 mg N/L at Peacock springs (median = 2.4 mg N/L). DOC and SO₄²⁻ concentrations range from 0.26 to 4.6 mg C/L (median = 0.49 mg C/L) and from 4.1 to 7.9 mg S/L (median = 7.6 mg S/L), respectively. Although we lack the TDN concentration for the sample with the highest NO₃⁻ concentration in this group, all other TDN concentrations were higher than the other two groups and range from 1.9 to 3.8 mg N/L (median = 2.7 mg N/L) and are at most ~ 0.4 mg N/L greater than NO₃⁻ concentrations ([Table 1](#)). These springs exhibit N₂O concentrations that range from 1.55 µg N/L (502% saturation) to 2.90 µg N/L (941% saturation) at Gilchrist Blue and Peacock springs, respectively ([Fig. 2](#)). Although N₂O concentrations were generally lower in samples with higher DO concentrations ([Fig. 4](#)), these variables are not significantly correlated. In contrast, NO₃⁻, DOC, and SO₄²⁻ concentrations increase with DO concentrations, although only the NO₃⁻-N₂O linear correlation is significant. The average EF values are similar but slightly lower than those of the Ichetucknee springs group. The EF_{NO3}⁻ values range from 0.0007 to 0.0015 (Eq. (1))

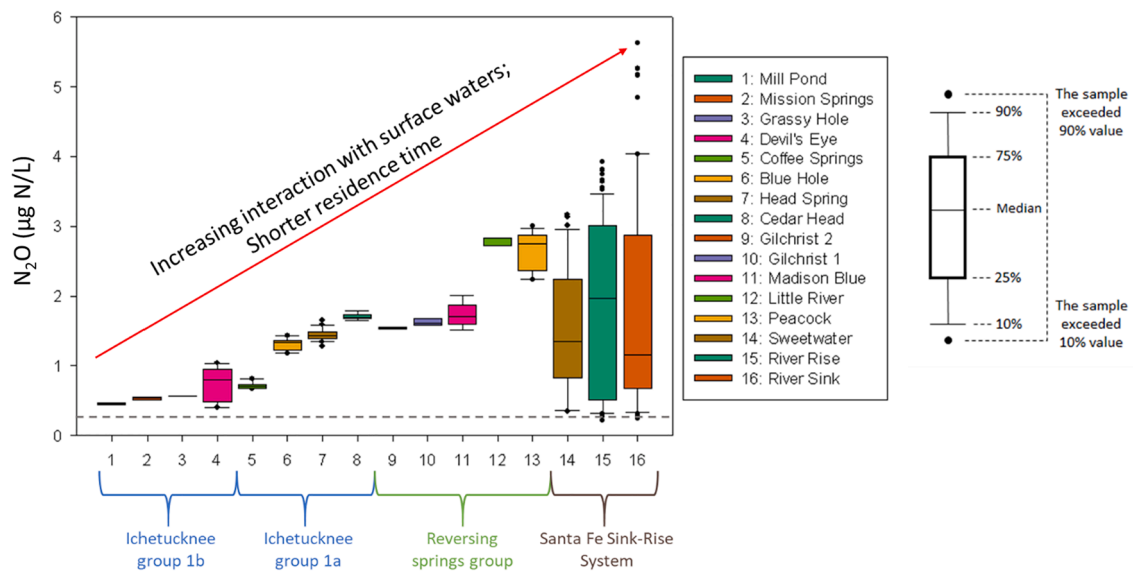


Fig. 2. Distribution of dissolved N_2O concentrations in springs discharging from the UFA. The dashed grey line represents water in equilibrium with global atmospheric N_2O (e.g., Weiss et al., 1980).

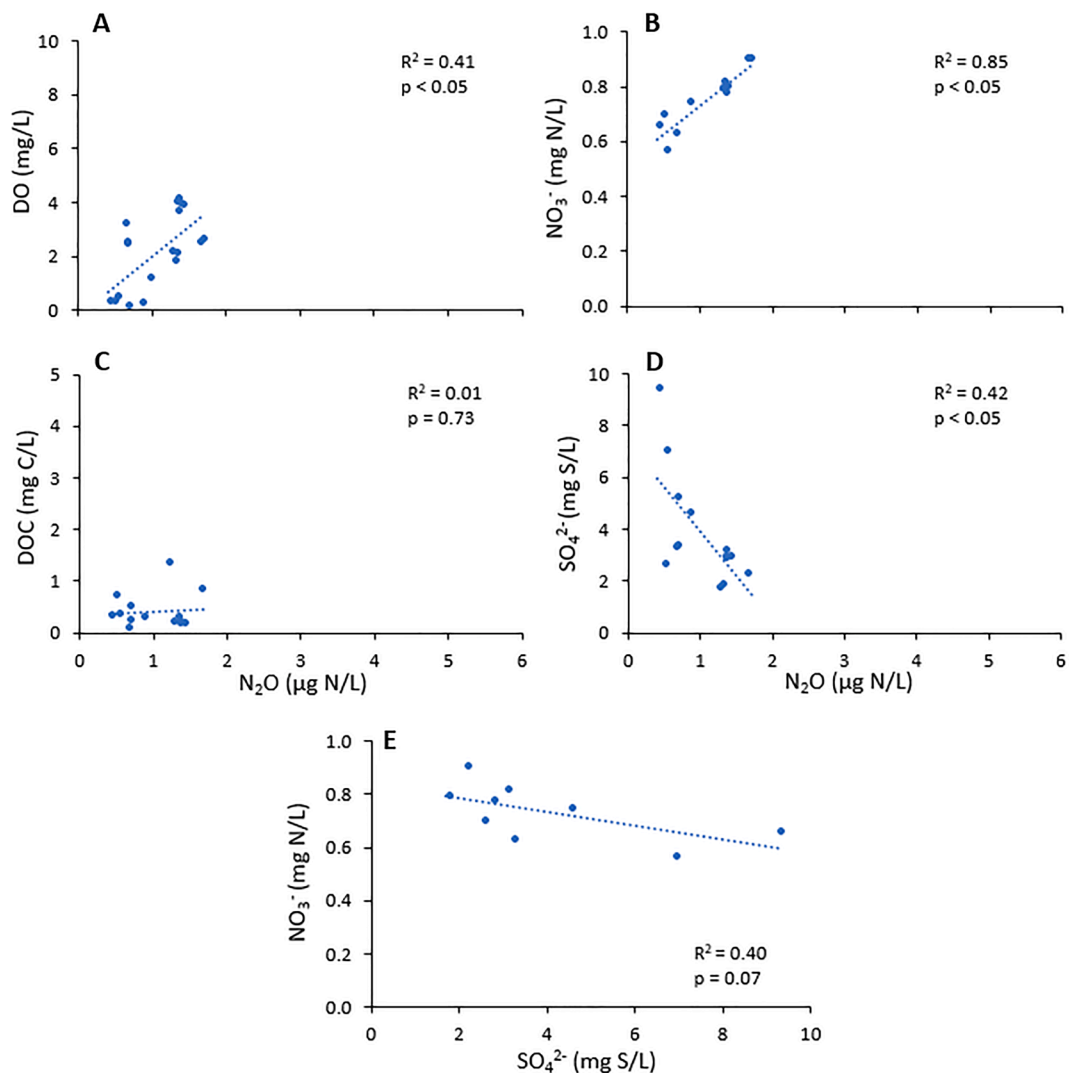


Fig. 3. N_2O vs. A. DO, B. NO_3^- , C. DOC, and D. SO_4^{2-} concentrations for the Ichetucknee springs system, and E. NO_3^- vs. SO_4^{2-} concentrations.

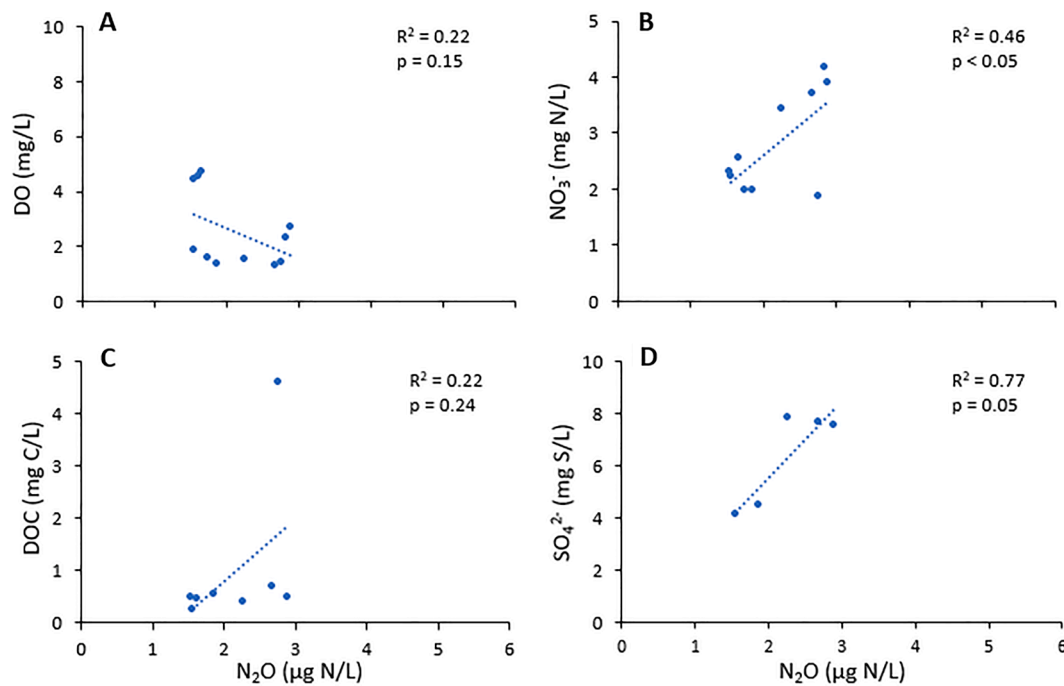


Fig. 4. N_2O vs. A. DO, B. NO_3^- , C. DOC, and D. SO_4^{2-} concentrations for the reversing springs group.

while the EF_{TDN} values range from 0.0006 to 0.0015 (Eq. (2)).

4.3. Santa Fe River Sink-Rise group

Water compositions at the Sink-Rise system show systematic variations from River Sink to River Rise that depend on discharge. Due to the continuous supply of surface water to the Sink-Rise system, it contains the highest DOC concentrations of all three spring groups. The Sink-Rise system also shows greater variance of all solute concentrations, including N_2O , compared to the other two spring groups (Fig. 2). SpC values range from 57.2 to 359.7 $\mu\text{S}/\text{cm}$ at River Sink, from 70.9 to 476.2 $\mu\text{S}/\text{cm}$ at Sweetwater Lake, and 69.3 to 526.0 $\mu\text{S}/\text{cm}$ at River Rise (Table 2). DO concentrations range from 2.61 to 9.30 mg/L at River Sink, from 0.96 to 7.83 mg/L at Sweetwater, and 0.65 to 7.16 mg/L at River Rise. Median NO_3^- concentrations increase from River Sink to River Rise, with concentrations of 0.12 mg N/L for River Sink, 0.20 mg N/L for Sweetwater Lake, and 0.23 mg N/L for River Rise. Unlike the other two spring groups, TDN concentrations within the Sink-Rise system reach up to ~ 9 times greater than NO_3^- concentrations, reflecting the presence of organic-N and/or other inorganic N_r species, such as NO_2^- and NH_4^+ . Assuming a molar C:N ratio of 50:1 for terrestrial derived organic-C (Perdue and Koprivnjak, 2007), a median DOC concentration for River Rise of 23.4 mg C/L indicates the presence of ~ 0.6 mg org-N/L, which indicates most of the excess TDN is organic N rather than NO_2^- or NH_4^+ , similar to the other spring groups. The highest DOC concentrations of all sample sites occur within the Sink-Rise system due to the continuous injection of surface water at River Sink, with median concentrations of 25.8 mg C/L for River Sink, 25.4 mg C/L for Sweetwater Lake, and 23.4 mg C/L for River Rise. Median SO_4^{2-} concentrations range from 3.3 mg S/L at River Sink, 6.4 mg S/L at Sweetwater Lake, and 11.5 mg S/L at River Rise. TDN concentrations at River Sink range from 0.2 to 1.3 mg N/L, from 0.4 to 1.1 mg N/L at Sweetwater, and from 0.3 to 1.2 mg N/L at River Rise.

Most samples from River Sink, Sweetwater Lake, and River Rise have N_2O concentrations that are supersaturated relative to the atmosphere, except during elevated discharge, when concentrations are near atmospheric equilibrium. Median N_2O concentrations increase from 1.14 μg N- $\text{N}_2\text{O}/\text{L}$ (370% saturation) at River Sink, to 1.36 μg N- $\text{N}_2\text{O}/\text{L}$ (441%

saturation) at Sweetwater, to 2.04 μg N- $\text{N}_2\text{O}/\text{L}$ (661% saturation) at River Rise Spring. This increase is up to ~ 2 μg N- $\text{N}_2\text{O}/\text{L}$ during most sampling times. In contrast with trends of increasing N_2O concentrations along the flow path, four sampling times had N_2O concentrations that decreased from River Sink to River Rise. These samples also contained the highest N_2O concentrations measured during this study, ranging from 3.45 to 5.09 μg N/L (1120% to 1738% saturation). Within the Sink-Rise system, significant positive correlations occur between N_2O and NO_3^- and SO_4^{2-} concentrations, while significant inverse correlations occur between N_2O and DO and DOC (Fig. 5). During base flow conditions, when discharge is greater at River Rise than River Sink, $\text{EF}_{\text{NO}_3^-}$ values varied more than 10-fold with time, ranging from 0.0032 to 0.0177 with a median value of 0.0086. The EF_{TDN} values are lower and range from 0.0007 to 0.0113 with a median value of 0.0042.

5. Discussion

Over the past ~ 50 years, NO_3^- concentrations are estimated to have risen by a factor of 50 in the UFA, from ≤ 0.1 mg N- $\text{NO}_3^- \text{L}^{-1}$ to values as high as 5 mg L^{-1} (Katz, 2004; Albertin et al., 2012). Increasing NO_3^- concentrations in the UFA have been traced back to multiple anthropogenic sources including fertilizer application (51%), animal waste (27%), septic tank drainage (12%), and natural atmospheric deposition (8%) (Katz et al., 2009). Nitrate was thought to have little or no attenuation in the UFA because of rapid flow combined with aerobic and organic carbon-poor conditions (Katz et al., 2009). This view has changed with observations of excess N_2 concentrations and stable isotope analyses of NO_3^- that indicate denitrification is widespread (Table 2) (Albertin et al., 2012; Heffernan et al., 2012; Henson et al., 2019). Therefore, our observations of N_2O in springs discharging from the UFA may reflect incomplete denitrification of NO_3^- to N_2O . Incomplete reduction of NO_3^- and accumulation of N_2O rather than N_2 has been documented in soils and groundwaters due to prevailing oxic conditions (Osaka et al., 2006; Laini et al., 2011; Jahangir et al., 2013; McAleer et al., 2017) and high NO_3^- concentrations that inhibit N_2O reduction to N_2 (Blackmer and Bremner, 1978; Weymann et al., 2008). However, the variations in N_2O concentrations observed in this study indicate that the extent of denitrification may differ across karst landscapes with variable

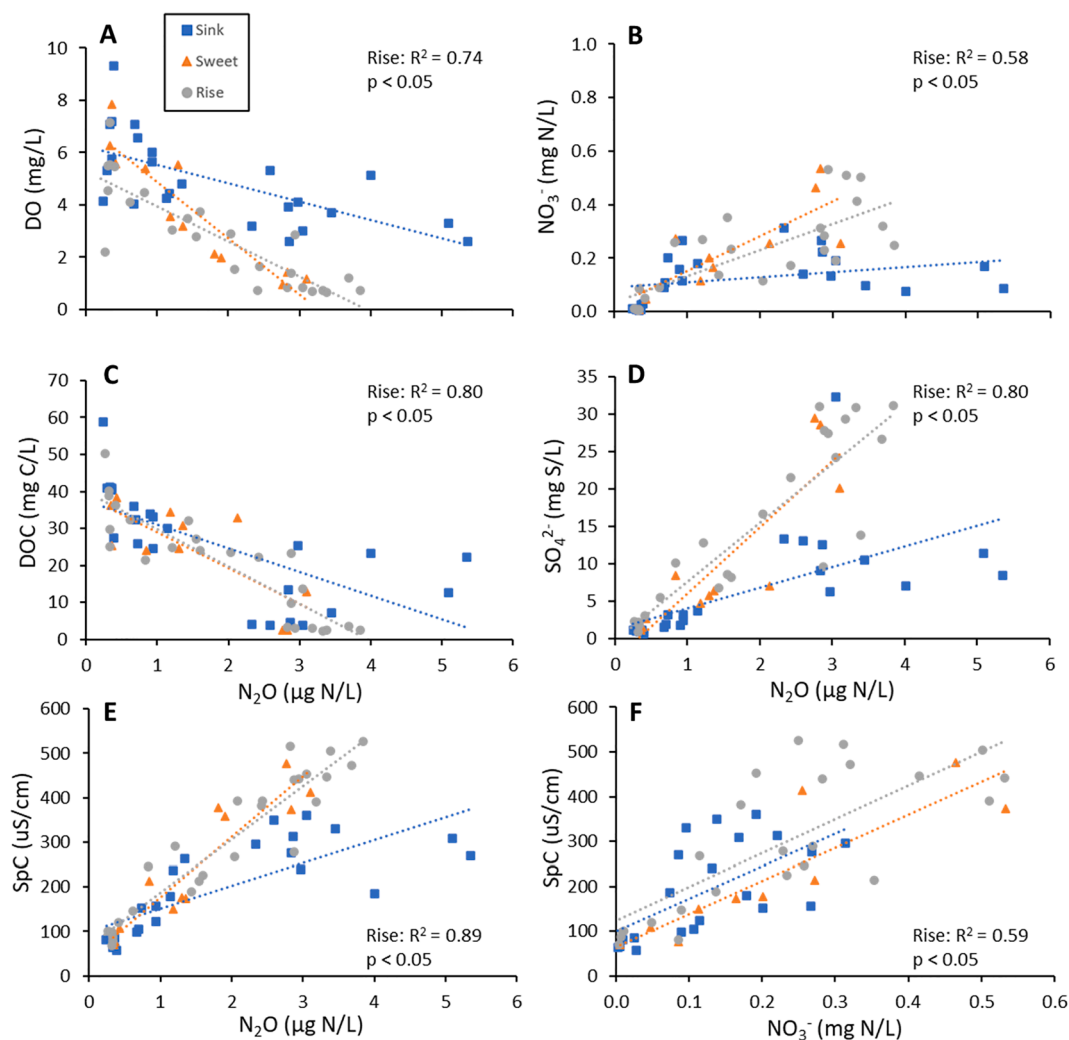


Fig. 5. N_2O vs. A. DO, B. NO_3^- , C. DOC, D. and SO_4^{2-} concentrations; SpC vs. E. N_2O , and F. NO_3^- concentrations at the Santa Fe River Sink-Rise system.

surface water-groundwater interactions, groundwater residence times, and availability of DOC. We evaluate these controls based on the spatial and temporal variations of water chemistry and N_2O concentrations.

5.1. N_2O sources

Despite variations in geochemical and hydrologic conditions among the three spring groups, all show a positive correlation between N_2O and NO_3^- concentrations, implying that elevated NO_3^- concentrations result in greater N_2O production. The NO_3^- - N_2O relationships differ between locations, however, the reversing springs group had the highest NO_3^- concentrations and the Sink-Rise system had the highest N_2O concentrations. These differences suggest factors other than NO_3^- concentrations contribute to the denitrification rate, and specifically, the reduction of NO_3^- and N_2O . Within the Ichetucknee springs group, up to 32% of available NO_3^- is denitrified to N_2 as reflected in excess N_2 concentrations measured in spring waters (Heffernan et al., 2012) (Table 2). These concentrations are about 3 orders of magnitude greater than the measured N_2O concentrations and suggest that within the Ichetucknee springs group, much, but not all NO_3^- is completely reduced to N_2 .

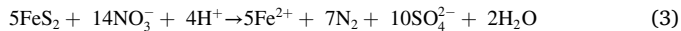
Although excess N_2 data are not available for the Sink-Rise system, the negative correlation between N_2O and DO and DOC concentrations (Fig. 5A, C) suggests denitrification may be the primary N_2O producing pathway. Identifying timing and locations of denitrification could be complicated by mixing of the surface water and groundwater if the two

sources have different N_2O concentrations. In addition to water recharging at River Sink, groundwater sources to River Rise are water draining from the matrix porosity to conduits at depths ~ 30 m below land surface and a second minor source from about 400 m below the land surface (Moore et al., 2009; Jin et al., 2015). This deep source is likely anoxic with negligible NO_3^- and N_2O concentrations, and thus unlikely to be a source of N_2O . We assume controls of N_2O concentrations are a result of shallow groundwater mixing with river water entering at River Sink coupled with production and consumption caused by varying redox conditions and rates of DOC remineralization within the matrix porosity (Fig. S2).

Distinguishing mixing from biogeochemical activity requires information on the mixing extent, which can be derived from conservative parameters such as SpC. Carbonate mineral dissolution increases groundwater SpC values by up to an order of magnitude more than river water (Gulley et al., 2011). The positive correlation between SpC values and NO_3^- and N_2O concentrations at River Rise (Fig. 5E-F) suggests draining of groundwater enriched in N_2O and NO_3^- relative to river water is a primary control on the N_2O concentrations at River Rise. Occasionally during base flow conditions, N_2O concentrations are elevated at River Sink compared to River Rise. These samples also contained the highest N_2O concentrations measured in this study (Fig. S2), were observed following long periods with no increases in river discharge, and represent an unknown source of N_2O production in the Santa Fe River headwaters.

The lack of correlation between N_2O and DOC in the Ichetucknee

springs group (Fig. 3A) opens the possibility that some of the N_2O could be produced by denitrifying microbes using inorganic electron donors such as reduced Fe, Mn and/or sulfur species. Nitrate reduction by pyrite has been documented in laboratory-based microbial incubations and flow-through experiments according to:



(Torrentó et al., 2010, 2011). This denitrification pathway is thermodynamically favorable and is hypothesized to be active across a range of geological and hydrological settings (Schwientek et al., 2008; Juncher Jørgensen et al., 2009; Zhang et al., 2009; Hayakawa et al., 2013). Pyrite is common in Suwannee Limestone of the UFA (Tihansky & Knochenmus, 2001), particularly in high-porosity zones (Price & Pichler, 2006) and oxidation of pyrite coupled to NO_3^- reduction is consistent with the inverse correlations between SO_4^{2-} and N_2O and NO_3^- concentrations within the Ichetucknee system (Fig. 3B & E). However, dissolution of gypsum in the Avon Park Formation, located a few hundred meters below land surface, may provide additional SO_4^{2-} to these waters (Miller 1986) without a corresponding reduction of NO_3^- . This source may be relevant to the Sink-Rise system considering its deep groundwater source (Moore et al., 2009; Jin et al., 2015). The SO_4^{2-} concentrations are greater in Ichetucknee group 1b springs than group 1a springs because of their greater depth of flow (Martin and Gordon, 2000), indicating the

possibility of a similar enrichment of SO_4^{2-} enrichment by gypsum dissolution in the Avon Park Formation. If the inverse correlation between N_2O and SO_4^{2-} concentrations reflects gypsum dissolution, then the poor correlation between N_2O and DOC may reflect DOC-remobilization through fermentation or the use of electron acceptors other than NO_3^- during the long subsurface residence times.

5.2. Residence time controls on N_2O dynamics

The length of time that water and associated reactants involved in nitrogen cycling reactions reside in the subsurface may control N_2O concentrations in spring waters. These potential drivers can be evaluated based on correlations between reactant and product concentrations. For example, such correlations have been used in a forested headwater catchment in Japan to show that shallow groundwater with high DO concentrations, presumably with short subsurface residence times, had elevated N_2O and NO_3^- concentrations, whereas deeper groundwater flow paths extending to anoxic portions of the aquifer allowed complete reduction to N_2 (Osaka et al., 2006). A similar relationship was found in a sandstone catchment (McAleer et al., 2017) in the Republic of Ireland, where N_2O concentrations were elevated under oxic to sub-oxic conditions (DO range 4–8 mg/L) and depleted under anoxic conditions (DO range 0–3 mg/L), where N_2 concentrations were

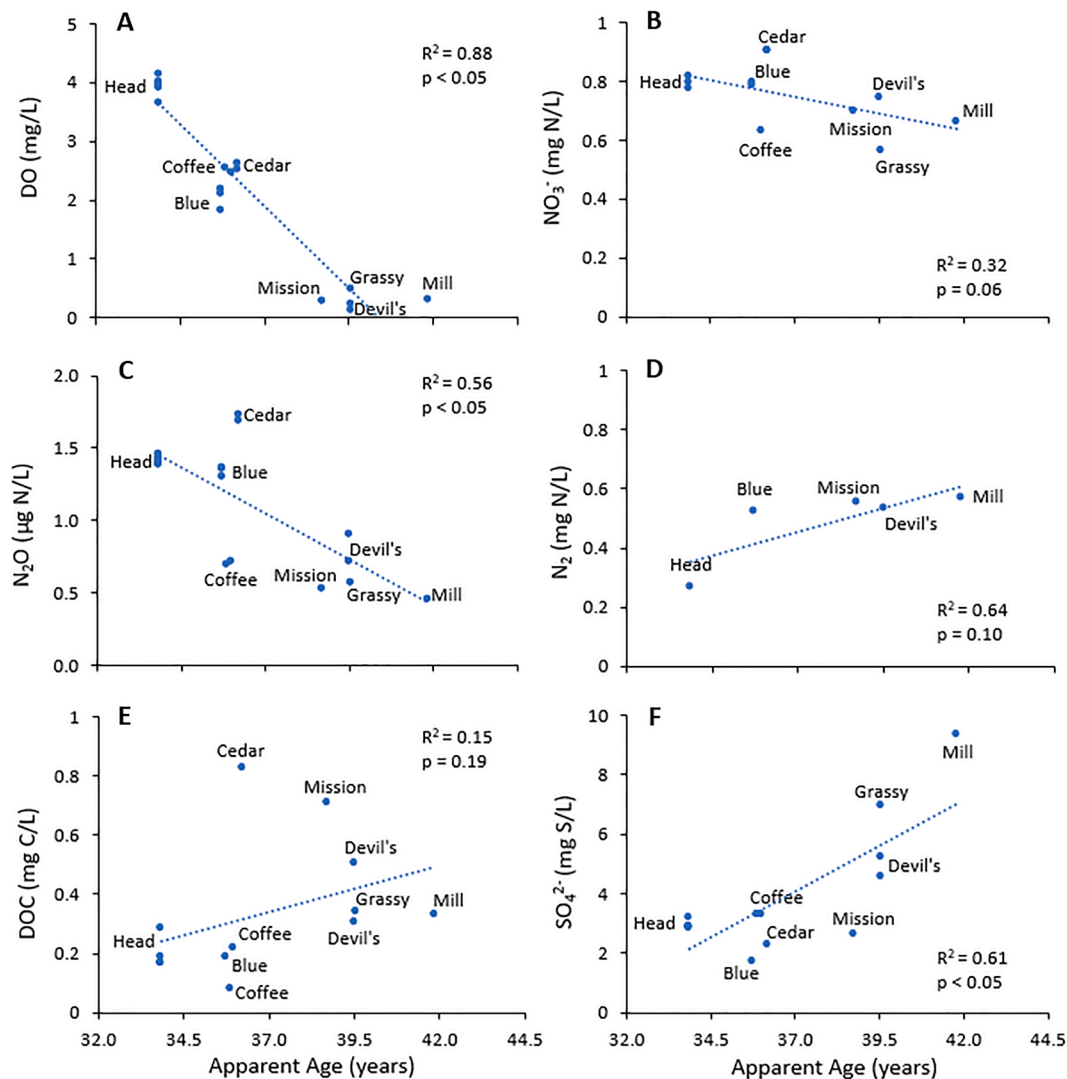


Fig. 6. Apparent age (Martin et al., 2016) versus A. DO, B. NO_3^- , C. N_2O , D. N_2 , E. DOC, and F. SO_4^{2-} concentrations in water discharging from the Ichetucknee springs group. N_2 data taken from Heffernan et al. (2012).

elevated. For the north-central Florida springs sampled here, the N_2O concentrations vary inversely across the spectrum of residence times (Fig. 2), with the lowest N_2O concentrations in the Ichetucknee springs with decades-long apparent ages for the discharging groundwater (Martin et al., 2016) and the highest, and also most variable, concentrations at the Santa Fe Sink-Rise system, where ground water has residence times of hours to days (Martin and Dean, 1999).

At Ichetucknee springs, lower N_2O concentrations in older spring waters of group 1b springs suggest more complete denitrification to N_2 (Table 2) than group 1a springs which have higher N_2O concentrations and younger apparent ages. The apparent ages of all springs show inverse correlations with DO, NO_3^- , and N_2O concentrations, which support increased reduction of DO, NO_3^- , and N_2O with longer residence times (Fig. 6A-C). Although not statistically significant, the apparent ages increase with increasing N_2 concentrations reported in Heffernan et al. (2012) for the Ichetucknee springs. If denitrification is the active N_2O producing mechanism, then these results suggest that longer subsurface residence times facilitate complete reduction of NO_3^- to N_2 (Fig. 6D).

Although the average age of Little River Spring (reversing springs group) water has been estimated to be ~ 21 years (Katz et al., 2001), at times following reversals, it should have shorter residence times on the order of weeks to months as river water intrudes and then discharges from the aquifer. Because the reversals also deliver elevated DO and DOC to the aquifer, these solutes would be expected to enhance N_2O production within the aquifer. The only water sampled from Little River Springs for this study was collected immediately after a reversal (Fig. S3) and showed an N_2O concentration of $2.76 \mu\text{g N-N}_2\text{O/L}$. This value is more than double the median value from the Ichetucknee springs group of $1.27 \mu\text{g N-N}_2\text{O/L}$, even though apparent ages of both springs are decades long. This greater concentration at Little River Spring suggests N_2O may have been produced during the reversal that occurred immediately prior to sampling or that cumulative effects of multiple reversals create geochemical conditions that are favorable for N_2O accumulation. None of the other springs within the reversing springs group was sampled immediately following a reversal, but nonetheless, their N_2O concentrations are up to 7 times greater than the minimum N_2O concentration observed within the Ichetucknee springs group. The elevated concentrations in the reversing springs group may thus reflect discharge of N_2O produced during the weeks to months that reversal water remains in the aquifer.

The short residence times for water flowing from River Sink to River Rise is modulated by gain or loss of water to or from the conduits as recharge into River Sink varies with river discharge. River Rise discharge ranged from 4 to $73 \text{ m}^3/\text{s}$ during sampling times and is commonly greater than discharge into River Sink. At residence times of approximately 17 h, conduits switch from gaining to losing water (Fig. 7). Longer residence times (up to ~ 72 h) occur during periods of low flow when River Rise discharge exceeds River Sink discharge, reflecting a gain of groundwater that is enriched in SpC, NO_3^- , N_2O , and SO_4^{2-} and low in DO and DOC concentrations. The estimated residence times show significant positive correlations with SpC, N_2O , NO_3^- , and SO_4^{2-} concentrations and significant negative correlations with DO and DOC concentrations (Fig. 8). The correlation between SpC and residence time (Fig. 8A) suggests that the primary control of variations in N_2O concentrations at River Rise stems from exchange of water between conduits and matrix porosity.

At intermediate residence times of 22 to 27 h that correspond to periods soon after conduits switch between gaining and losing water (Fig. 7), N_2O concentrations are anomalously high relative to the linear correlations with residence time at River Rise (Fig. 8D; circled data points). The correspondence of increased N_2O concentrations at times when DOC- and DO-rich surface waters are delivered to the NO_3^- rich groundwater within the matrix porosity suggests that N_2O production is enhanced by the exchange of water between the conduits and the surrounding matrix porosity, similar to production of N_2O following spring

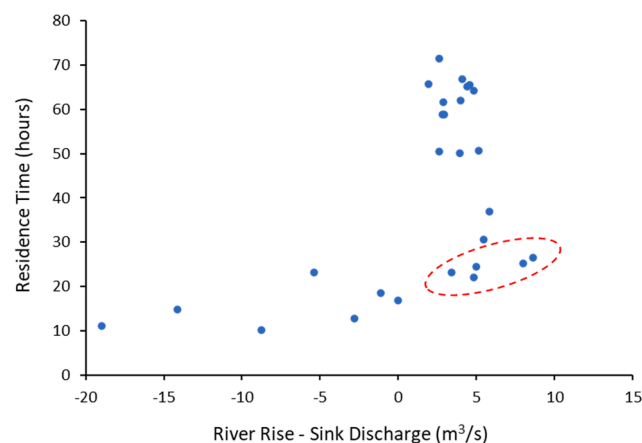


Fig. 7. River Rise minus River Sink discharge versus residence time of allogenic water discharging at River Rise. Where River Rise minus River Sink discharge is negative, allogenic conduit water flows into the matrix porosity to the conduits and where positive water flows from the matrix porosity to conduits. The data points circled in dashed-red (~ 22 – 27 h) are those immediately following matrix recharge events and correspond approximately with increased N_2O and NO_3^- concentrations observed at River Rise.

reversals. Because of the limited amount of time (hours to days) that the recharged river water resides within the matrix porosity, complete denitrification to N_2 may not occur, as supported by the linear increase in N_2O concentrations with increasing residence time at River Rise (Fig. 8D).

5.3. N_2O emission factors

N_2O concentrations in discharging spring waters depend on the extent of N_r reduction (NO_3^-) and/or oxidation (NH_4^+) to N_2O within the aquifer and is commonly evaluated based on emission factor estimates (e.g., IPCC, Hergoualc'h et al., 2019). Emission factors for aquatic ecosystems are divided into three categories depending on the environment and include groundwater, streams and rivers, and estuaries, the most relevant value of which for comparison to the north-central Florida springs is the groundwater emission factor (EF_{5g}). Estimates of global groundwater EF values have changed by nearly a factor of ten over the recent decades, reflecting the difficulty associated with estimating this value. The most recently reported mean EF_{5g} value is 0.0060 (Tian et al., 2019) based on 101 studies of agriculturally impacted groundwater and springs (avg. $EF_{5g} = 0.0079$), as well as upstream or surface water drainage (avg. $EF_{5g} = 0.0040$). Uncertainties in groundwater emission factors arise from the complex subsurface dynamics in aquifers and heterogeneous production, reduction, and transport mechanisms of N_2O . These uncertainties contribute to poorly constrained values for the atmospheric evasion of N_2O from aquatic systems (Yao et al., 2020). Atmospheric evasion from numerous locations around the world are influenced by spring discharge as reflected by decreasing concentrations of N_2O downstream from springs sources (Ueda et al., 1993; Osaka et al., 2006). Furthermore, N_2O evasion from springs are 60 to 100 times greater than N_2O evasion from surrounding soils (Osaka et al., 2006; Hedlund et al., 2011). Evaluation of karst groundwater EF values may thus help constrain the potential for atmospheric evasion of N_2O from spring waters.

The average groundwater EF_{NO_3} (Eq. (1)) values for the sampled north-central Florida springs is $0.0045 \text{ mg N-N}_2\text{O}/\text{mg N-NO}_3^-$ but they show a large range from lows of 0.0007 in the Ichetucknee springs and reversing springs groups to as high as 0.0177 for the Santa Fe River Rise. The average EF value for north-central Florida springs is heavily weighted by elevated groundwater EF values estimated for River Rise, supporting N_2O production caused by continuous delivery at River Sink of reactants (e.g., DOC, DO, and NO_3^-) to the subsurface involved in

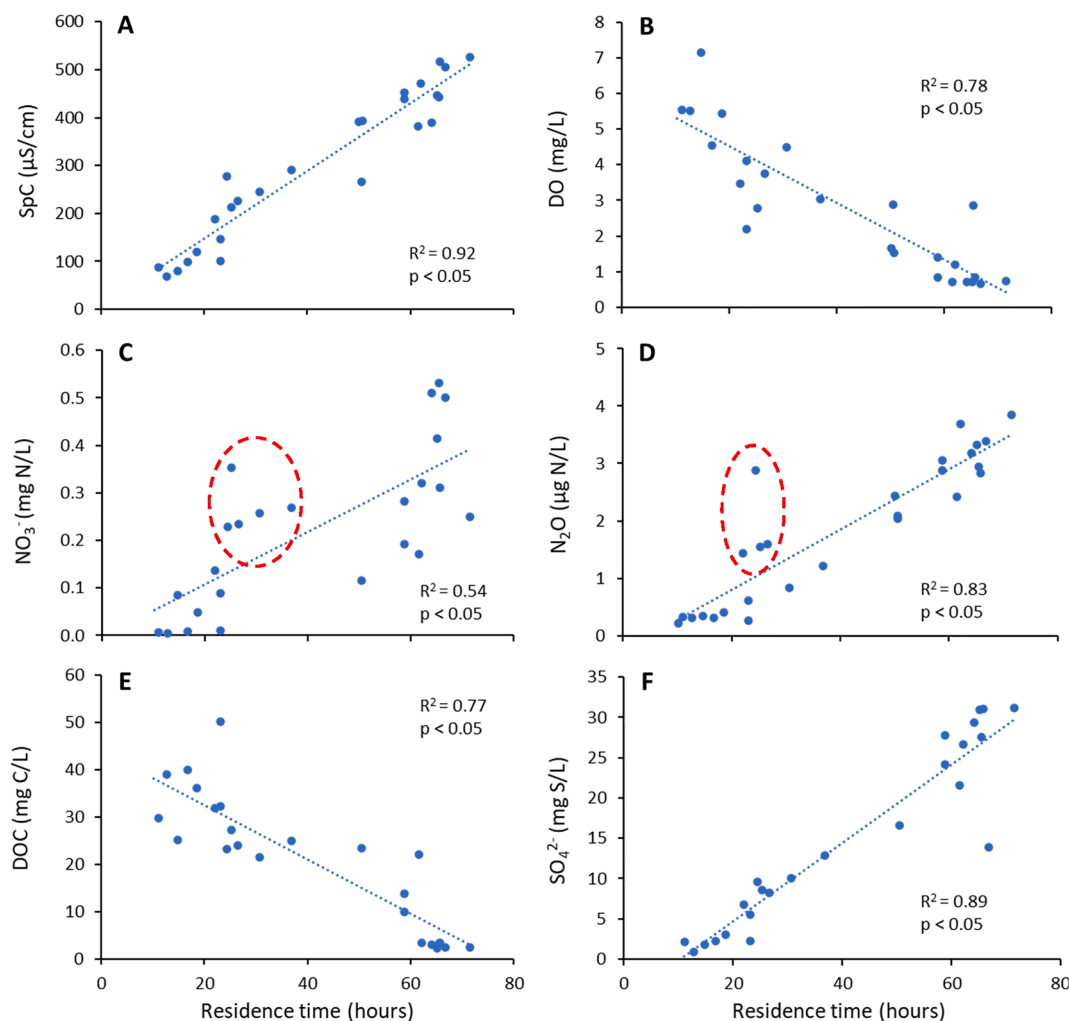


Fig. 8. Relationship of SpC, DO, NO_3^- , N_2O , DOC, and SO_4^{2-} concentrations with apparent subsurface residence time of allogenic River Sink water discharging from River Rise. Sample points circled in dashed-red represent spikes in NO_3^- and N_2O concentrations correlating with residence times indicated in Fig. 7 (also circled in dashed-red).

nitrogen cycling. However, the highest EF values occur at River Sink with $\text{EF}_{\text{NO}_3^-}$ values of 0.0627 and EF_{TDN} (Eq. (2)) values of 0.0131. These high EF values for the River Sink water suggest greater reduction and/or oxidation of N_r species to N_2O in surface waters draining from landscapes in the Santa Fe River headwaters. Here, the UFA is semi-confined versus the other spring groups where N_2O reduction may be more prominent as shown by low EF factors at the reversing springs and Ichetucknee springs groups (Table 1). The semi-confined nature of the region upstream of River Sink suggests additional groundwater-surface water exchange resulting in N_2O production during certain flow conditions, similar to the production between River Sink and River Rise. Because most of the UFA springs have EF values much lower than the global average, the Floridan aquifer appears to have a lower potential to contribute N_2O to surface waters. This low potential for N_2O contribution may be common to other anthropogenically impacted eogenetic karst aquifers in addition to the UFA due to spring waters that typically have residence times on the order of years to decades (Florea and Vacher, 2006). While the presence of elevated NO_3^- concentrations is inherently required for N_2O production, these results suggest that the turnover of NO_3^- to N_2O in anthropogenically impacted eogenetic karst aquifers with high NO_3^- concentrations is ultimately controlled by the amount of DOC and DO delivered to the subsurface, facilitated by surface-groundwater interactions.

6. Conclusions

All of the UFA springs sampled in this study had N_2O concentrations that are supersaturated compared to equilibrium with atmospheric concentrations, with saturations reaching up to ~1250%. N_2O concentrations increase with increasing connectivity between surface water and groundwater that enhances the input of DOC into the subsurface, fueling denitrification. N_2O concentrations are lower where the discharging water has residence times on the order of decades, as represented by the Ichetucknee springs and reversing springs groups, in comparison to spring water with residence times on the order of hours to days as represented by the Sink-Rise system. The low concentrations in older spring water likely reflect reduction of a larger portion of the N_2O to N_2 , which is consistent with groundwater EF values for the Ichetucknee and reversing springs groups that are about an order of magnitude lower than the newly refined global average for groundwater of 0.0060 (Tian et al., 2019). In contrast, median groundwater EF values are around 5 times greater where residence times are short as exemplified by the Sink-Rise system. At that location, N_2O concentrations increase as residence times increase from several hours to several days with decreasing discharge, and is a result of continuous input of DOC and DO-rich surface waters into the system. These results imply that the initial input of redox sensitive solutes and subsequent subsurface processing times affect N_2O fluxes from karst aquifers, with longer residence times facilitating further reduction of N_2O to N_2 prior to

discharging to the surface.

CRedit authorship contribution statement

Madison K. Flint: Conceptualization, Validation, Formal analysis, Investigation, Writing - original draft, Writing - review & editing, Visualization. **Jonathan B. Martin:** Conceptualization, Resources, Writing - original draft, Writing - review & editing, Supervision. **Tatiana I. Summerall:** Investigation, Writing - original draft. **Adrian Barry-Sosa:** Conceptualization, Investigation, Writing - original draft, Writing - review & editing. **Brent C. Christner:** Conceptualization, Resources, Writing - original draft, Writing - review & editing, Supervision.

Declaration of Competing Interest

The authors declare that they have no known competing financial interests or personal relationships that could have appeared to influence the work reported in this paper.

Acknowledgements

This material is based upon work supported by the National Science Foundation under grant No. EAR 1740481 and support from UFBI Seed grant #020518. The authors would like to thank Christine Housel for granting permit #06281812 and #03211912A and the Florida State Parks for allowing us to collect samples. The authors would also like to thank both current and past undergraduate students who have helped tremendously with sample collection: Joshua Solt and Krista Van Der Velde.

Appendix A. Supplementary data

Supplementary data to this article can be found online at <https://doi.org/10.1016/j.jhydrol.2020.125936>.

References

- Albertin, A.R., Sickman, J.O., Pinowska, A., Stevenson, R.J., 2012. Identification of nitrogen sources and transformations within karst springs using isotope tracers of nitrogen. *Biogeochemistry* 108, 219–232. <https://doi.org/10.1007/s10533-011-9592-0>.
- Bailly-Comte, V., Martin, J.B., Jourde, H., Scream, E.J., Pistre, S., Langston, A., 2010. Water exchange and pressure transfer between conduits and matrix and their influence on hydrodynamics of two karst aquifers with sinking streams. *J. Hydrol.* 386, 55–66. <https://doi.org/10.1016/j.jhydrol.2010.03.005>.
- Bailly-Comte, V., Martin, J.B., Scream, E.J., 2011. Time variant cross correlation to assess residence time of water and implication for hydraulics of a sink-rise karst system. *Water Resour. Res.* 47 <https://doi.org/10.1029/2010WR009613>.
- Blackmer, A.M., Bremner, J.M., 1978. Inhibitory effect of nitrate on reduction of N₂O to N₂ by soil microorganisms. *Soil Biol. Biochem.* 10, 187–191. [https://doi.org/10.1016/0038-0717\(78\)90095-0](https://doi.org/10.1016/0038-0717(78)90095-0).
- Brown, A.L., Martin, J.B., Scream, E.J., Ezell, J.E., Spellman, P., Gulley, J., 2014. Bank storage in karst aquifers: the impact of temporary intrusion of river water on carbonate dissolution and trace metal mobility. *Chem. Geol.* 385, 56–69. <https://doi.org/10.1016/j.chemgeo.2014.06.015>.
- Brown, A.L., Martin, J.B., Kamenov, G.D., Ezell, J.E., Scream, E.J., Gulley, J., Spellman, P., 2019. Trace metal cycling in karst aquifers subject to periodic river water intrusion. *Chem. Geol.* 527, 118773. <https://doi.org/10.1016/j.chemgeo.2018.05.020>.
- Butterbach-Bahl, K., Baggs, E.M., Dannenmann, M., Kiese, R., Zechmeister-Boltenstern, S., 2013. Nitrous oxide emissions from soils: How well do we understand the processes and their controls? *Philosophical Transactions of the Royal Society B: Biological Sciences*. DOI:10.1098/rstb.2013.0122.
- Cohen, M.J., Heffernan, J.B., Albertin, A., Martin, J.B., 2012. Inference of riverine nitrogen processing from longitudinal and diel variation in dual nitrate isotopes. *J. Geophys. Res. Biogeosci.* 117 <https://doi.org/10.1029/2011JG001715>.
- Cooper, R.J., Wexler, S.K., Adams, C.A., Hiscock, K.M., 2017. Hydrogeological controls on regional-scale indirect nitrous oxide emission factors for rivers. *Environ. Sci. Technol.* 51, 10440–10448. <https://doi.org/10.1021/acs.est.7b02135>. <https://doi.org/10.1021/acs.est.7b02135.s00110>. <https://doi.org/10.1021/acs.est.7b02135.s002>.
- Davidson, E.A., Kanter, D., 2014. Inventories and scenarios of nitrous oxide emissions. *Environ. Res. Lett.* 9, 105012. <https://doi.org/10.1088/1748-9326/9/10/105012>.
- Florea, L.J., Vacher, H.L., 2006. Springflow hydrographs: Eogenetic vs Telogenetic Karst. *Groundwater* 44 (3), 352–361. <https://doi.org/10.1111/gwat.2006.44.issue-310.1111/j.1745-6584.2005.00158.x>.
- Ford, D. C., & Williams, P. W., 2007. *Karst Hydrology and Geomorphology*. Chichester, UK: Wiley.
- Galloway, J.N., Cowling, E.B., 2002. Reactive nitrogen and the world: 200 Years of change, in: *Ambio*. Royal Swedish Academy of Sciences, pp. 64–71. DOI:10.1579/0044-7447-31.2.64.
- Galloway, J.N., Dentener, F.J., Capone, D.G., Boyer, E.W., Howarth, R.W., Seitzinger, S. P., Asner, G.P., Cleveland, C.C., Green, P.A., Holland, E.A., Karl, D.M., Michaels, A. F., Porter, J.H., Townsend, A.R., Vörösmarty, C.J., 2004. Nitrogen Cycles: Past, Present, and Future. *Biogeochemistry* 70, 153–226.
- Galloway, J.N., Townsend, A.R., Erisman, J.W., Bekunda, M., Cai, Z., Freney, J.R., Martinelli, L.A., Seitzinger, S.P., Sutton, M.A., 2008. Transformation of the nitrogen cycle: recent trends, questions, and potential solutions. *Science* 320, 889–892. <https://doi.org/10.1126/science.1136674>.
- Goldscheider, N., Chen, Z., Auler, A.S., Bakalowicz, M., Broda, S., Drew, D., Hartmann, J., Jiang, G., Moosdorf, N., Stevanovic, Z., Veni, G., 2020. Global distribution of carbonate rocks and karst water resources. *Hydrogeol. J.* 1661–1677. <https://doi.org/10.1007/s10040-020-02139-5>.
- Gulley, J., Martin, J.B., Scream, E.J., Moore, P.J., 2011. River reversals into karst springs: a model for cave enlargement in eogenetic karst aquifers. *Bull. Geol. Soc. Am.* 123, 457–467. <https://doi.org/10.1130/B30254.1>.
- Hayakawa, A., Hatakeyama, M., Asano, R., Ishikawa, Y., Hidaka, S., 2013. Nitrate reduction coupled with pyrite oxidation in the karst sediments of a sulfide-rich ecosystem. *J. Geophys. Res. Biogeosci.* 118, 639–649. <https://doi.org/10.1002/jgrg.20060>.
- Hedlund, B.P., McDonald, A.I., Lam, J., Dodsworth, J.A., Brown, J.R., Hungate, B.A., 2011. Potential role of *Thermus thermophilus* and *T. oshimai* in high rates of nitrous oxide (N₂O) production in ~80°C hot springs in the US Great Basin. *Geobiology* 9, 471–480. <https://doi.org/10.1111/j.1472-4669.2011.00295.x>.
- Heffernan, J.B., Albertin, A.R., Fork, M.L., Katz, B.G., Cohen, M.J., 2012. Denitrification and inference of nitrogen sources in the karstic Floridan Aquifer. *Biogeochemistry* 9, 1671–1690. <https://doi.org/10.5194/bg-9-1671-2012>. <https://doi.org/10.5194/bg-9-1671-2012-supplement>.
- Henson, W.R., Cohen, M.J., Graham, W.D., 2019. Spatially distributed denitrification in a karst springshed. *Hydro. Process.* 33, 1191–1203. <https://doi.org/10.1002/hyp.v33.810.1002/hyp.13380>.
- Hergoualc'h, K., Akiyama, H., Bernoux, M., Chirinda, N., del Prado, A., Kasimir, Å., MacDonald, J., Ogle, S., Regina, K., van der Weerden, T., 2019. Chapter 11: N₂O Emissions from Managed Soils, and CO₂ Emissions from Lime and Urea Application. In: 2019 Refinement to the 2006 IPCC Guidelines for National Greenhouse Gas Inventories.
- Hiscock, K.M., Bateman, A.S., Mühlherr, I.H., Fukada, T., Dennis, P.F., 2003. Indirect emissions of nitrous oxide from regional aquifers in the United Kingdom. *Environ. Sci. Technol.* 37, 3507–3512. <https://doi.org/10.1021/es020216w>.
- Jahangir, M.M.R., Johnston, P., Barrett, M., Khalil, M.I., Groffman, P.M., Boeckx, P., Fenton, O., Murphy, J., Richards, K.G., 2013. Denitrification and indirect N₂O emissions in groundwater: hydrologic and biogeochemical influences. *J. Contam. Hydrol.* 152, 70–81. <https://doi.org/10.1016/j.jconhyd.2013.06.007>.
- Jin, J., Zimmerman, A.R., Martin, J.B., Khadka, M.B., 2015. Spatiotemporal variations in carbon dynamics during a low flow period in a carbonate karst watershed: Santa Fe River, Florida, USA. *Biogeochemistry* 122, 131–150. <https://doi.org/10.1007/s10533-014-0035-6>.
- Juncher Jørgensen, C., Jacobsen, O.S., Elberling, B.o., Aamand, J., 2009. Microbial oxidation of pyrite coupled to nitrate reduction in anoxic groundwater sediment. *Environ. Sci. Technol.* 43, 4851–4857. <https://doi.org/10.1021/es803417s>.
- Jurado, A., Borges, A.V., Pujades, E., Briens, P., Nikolenko, O., Dassargues, A., Brouyère, S., 2018. Dynamics of greenhouse gases in the river-groundwater interface in a gaining river stretch (Triffroy catchment, Belgium). *Hydrogeol. J.* 26, 2739–2751. <https://doi.org/10.1007/s10040-018-1834-y>.
- Katz, B.G., 2004. Sources of nitrate contamination and age of water in large karstic springs of Florida. *Environ. Geol.* 46, 689–706. <https://doi.org/10.1007/s00254-004-1061-9>.
- Katz, B.G., Böhlke, J.K., Hornsby, H.D., 2001. Timescales for nitrate contamination of spring waters, northern Florida, USA. *Chem. Geol.* 179, 167–186. [https://doi.org/10.1016/S0009-2541\(01\)00321-7](https://doi.org/10.1016/S0009-2541(01)00321-7).
- Katz, B.G., Sepulveda, A.A., Verdi, R.J., 2009. Estimating nitrogen loading to ground water and assessing vulnerability to nitrate contamination in a large karstic springs Basin, Florida. *J. Am. Water Resour. Assoc.* 45, 607–627. <https://doi.org/10.1111/j.1752-1688.2009.00309.x>.
- Laini, A., Bartoli, M., Castaldi, S., Viaroli, P., Capri, E., Trevisan, M., 2011. Greenhouse gases (CO₂, CH₄ and N₂O) in lowland springs within an agricultural impacted watershed (Po River Plain, northern Italy). *Chem. Ecol.* 27, 177–187. <https://doi.org/10.1080/02757540.2010.547489>.
- Martin, J.B. and Gordon, S.L., 2000. Surface and ground water mixing, flow paths, and temporal variations in chemical compositions of karst springs. In: Sasowsky, I.D., Wicks, C. (Eds.), *Groundwater Flow and Contaminant Transport in Carbonate Aquifers*. A.A. Balkema, Rotterdam, pp. 65–92.
- Martin, J.B., Dean, R., 1999. Temperature as a natural tracer of short residence times for groundwater in karst aquifers. *Karst Modeling: Karst Waters Inst. Spec. Publ.* 5, 236–242.
- Martin, J.B., Kurz, M.J., Khadka, M.B., 2016. Climate control of decadal-scale increases in apparent ages of eogenetic karst spring water. *J. Hydrol.* 540, 988–1001. <https://doi.org/10.1016/j.jhydrol.2016.07.010>.
- McAleer, E.B., Coxon, C.E., Richards, K.G., Jahangir, M.M.R., Grant, J., Mellander, P.E., 2017. Groundwater nitrate reduction versus dissolved gas production: a tale of two catchments. *Sci. Total Environ.* 586, 372–389. <https://doi.org/10.1016/j.scitotenv.2016.11.083>.

- Miller, J.A., 1986. Hydrogeologic Framework of the Floridan Aquifer System in Florida and in Parts of Georgia, Alabama, and South Carolina. U.S. Geological Survey Professional Paper 1403-E.
- Moore, P.J., Martin, J.B., Sreaton, E.J., 2009. Geochemical and statistical evidence of recharge, mixing, and controls on spring discharge in an eogenetic karst aquifer. *J. Hydrol.* 376, 443–455. <https://doi.org/10.1016/j.jhydrol.2009.07.052>.
- Mühlherr, I.H., Hiscock, K.M., 1998. Nitrous oxide production and consumption in British limestone aquifers. *J. Hydrol.* 211, 126–139.
- Myhre, G., D. Shindell, F.-M. Bréon, W. Collins, J. Fuglestedt, J. Huang, D. Koch, J.-F. Lamarque, D. Lee, B. Mendoza, T. Nakajima, A. Robock, G. Stephens, T. Takemura and H. Zhang, 2013. Chapter 8, Anthropogenic and Natural Radiative Forcing. In: *Climate Change 2013: The Physical Science Basis. Contribution of Working Group I to the Fifth Assessment Report of the Intergovernmental Panel on Climate Change* [Stocker, T.F., D. Qin, G.-K. Plattner, M. Tignor, S.K. Allen, J. Boschung, A. Nauels, Y. Xia, V. Bex and P.M. Midgley (eds.)]. Cambridge University Press, Cambridge, United Kingdom and New York, NY, USA.
- Osaka, K., Ohte, N., Koba, K., Katsuyama, M., Nakajima, T., 2006. Hydrologic controls on nitrous oxide production and consumption in a forested headwater catchment in central Japan. *J. Geophys. Res. Biogeosci.* 111 <https://doi.org/10.1029/2005JG000026>.
- Pain, A.J., Martin, J.B., Young, C.R., 2019. Sources and sinks of CO₂ and CH₄ in siliciclastic subtropical estuaries. *Limnol. Oceanogr.* 64, 1500–1514. <https://doi.org/10.1002/lno.v64.410.1002/lno.11131>.
- Perdue, E.M., Koprivnjak, J.-F., 2007. Using the C/N ratio to estimate terrigenous inputs of organic matter to aquatic environments. *Estuar. Coast. Shelf Sci.* 73 (1–2), 65–72.
- Price, R.E., Pichler, T., 2006. Abundance and mineralogical association of arsenic in the Suwannee Limestone (Florida): implications for arsenic release during water-rock interaction. *Chem. Geol.* 228, 44–56. <https://doi.org/10.1016/j.chemgeo.2005.11.018>.
- Puri, H. S. and Vernon, R. O., 1964. Summary of the Geology of Florida and a Guidebook to the Classic Exposures. Florida Geological Survey Special Publication #5.
- Ravishankara, A.R., Daniel, J.S., Portmann, R.W., 2009. Nitrous oxide (N₂O): the dominant ozone-depleting substance emitted in the 21st century. *Science* 326, 123–125. <https://doi.org/10.1126/science.1176985>.
- Repo, E., Huttunen, J.T., Naumov, A.V., Chichulin, A.V., Lapshina, E.D., Bleuten, W., Martikainen, P.J., 2007. Release of CO₂ and CH₄ from small wetland lakes in western Siberia. *Tellus B: Chem. Phys. Meteorol.* 59, 788–796. <https://doi.org/10.1111/j.1600-0889.2007.00301.x>.
- Ritorto, M., Sreaton, E.J., Martin, J.B., Moore, P.J., 2009. Relative importance of chemical effects of diffuse and focused recharge in an eogenetic karst aquifer: an example from the unconfined upper Floridan aquifer, USA. *Hydrogeol. J.* 17, 1687–1698. <https://doi.org/10.1007/s10040-009-0460-0>.
- Rosenau, J.C., Faulkner, G.L., Hendry Jr., C.W., Hull, R.W., 1977. Springs of Florida. *Fla. Bur. Geol. Bull.* 31 (revised).
- Schwientek, M., Einsiedl, F., Stichler, W., Stögbauer, A., Strauss, H., Maloszewski, P., 2008. Evidence for denitrification regulated by pyrite oxidation in a heterogeneous porous groundwater system. *Chem. Geol.* 255, 60–67. <https://doi.org/10.1016/j.chemgeo.2008.06.005>.
- Scott, T.M., Means, G.H., Means, R.C. and Meegan, R.P., 2002. First Magnitude Springs of Florida. Open File Report Rep. No. 85, Florida Geological Survey, Tallahassee, Florida.
- Sutton, J.E., Sreaton, E.J., Martin, J.B., 2015. Insights on surface-water/groundwater exchange in the upper Floridan aquifer, north-central Florida (USA), from streamflow data and numerical modeling. *Hydrogeol. J.* 23, 305–317. <https://doi.org/10.1007/s10040-014-1213-2>.
- Thomson, A.J., Giannopoulos, G., Pretty, J., Baggs, E.M., Richardson, D.J., 2012. Biological sources and sinks of nitrous oxide and strategies to mitigate emissions. *Phil. Trans. R. Soc. B* 367, 1157–1168. <https://doi.org/10.1098/rstb.2011.0415>.
- Tian, L., Cai, Y., Akiyama, H., 2019. A review of indirect N₂O emission factors from agricultural nitrogen leaching and runoff to update the default IPCC values. *Environ. Pollut.* 245, 300–306. <https://doi.org/10.1016/j.envpol.2018.11.016>.
- Tihansky, A. B., and Knochenmus, L. A., 2001. Karst Features and Hydrogeology in West-Central Florida - A Field Perspective. in: Kuniandy, E.L. (ed.) U.S. Geological Survey Karst Interest Group Proceedings. USGS Water-Resources Investigations Report 01-4011.
- Torrentó, C., Cama, J., Urmeneta, J., Otero, N., Soler, A., 2010. Denitrification of groundwater with pyrite and Thiobacillus denitrificans. *Chem. Geol.* 278, 80–91. <https://doi.org/10.1016/j.chemgeo.2010.09.003>.
- Torrentó, C., Urmeneta, J., Otero, N., Soler, A., Viñas, M., Cama, J., 2011. Enhanced denitrification in groundwater and sediments from a nitrate-contaminated aquifer after addition of pyrite. *Chem. Geol.* 287, 90–101. <https://doi.org/10.1016/j.chemgeo.2011.06.002>.
- Ueda, S., Ogura, N., Yoshinari, T., 1993. Accumulation of nitrous oxide in aerobic groundwaters. *Wat. Res.* 27 (12), 1787–1792.
- Vacher, H.L., Mylroie, J.E., 2002. Eogenetic karst from the perspective of an equivalent porous medium. *Carbonates Evaporites* 17, 182–196.
- Weiss, R.F., Price, B.A., Canada, E., Rochette, P., Hutchinson, G.L., Jayasundara, S., Wagner-Riddle, C., 1980. Nitrous oxide solubility in water and seawater. *Agric. Syst.* 8, 247–286. <https://doi.org/10.1017/CBO9781107415324.004>.
- Weymann, D., Well, R., Flessa, H., von der Heide, C., Deurer, M., Meyer, K., Konrad, C., Walther, W., 2008. Groundwater N₂O emission factors of nitrate-contaminated aquifers as derived from denitrification progress and N₂O accumulation. *Biogeosciences* 5, 1215–1226. <https://doi.org/10.5194/bg-5-1215-2008>.
- Yang, M., Antonio Yaquian, J., Annable, M.D., Jawitz, J.W., 2019. Karst conduit contribution to spring discharge and aquifer cross-sectional area. *J. Hydrol.* 578, 124037 <https://doi.org/10.1016/j.jhydrol.2019.124037>.
- Yao, Y., Tian, H., Shi, H., Pan, S., Xu, R., Pan, N., Canadell, J.G., 2020. Increased global nitrous oxide emissions from streams and rivers in the Anthropocene. *Nat. Clim. Change* 10, 138–142. <https://doi.org/10.1038/s41558-019-0665-8>.
- Zhang, Y.C., Slomp, C.P., Broers, H.P., Passier, H.F., van Cappellen, P., 2009. Denitrification coupled to pyrite oxidation and changes in groundwater quality in a shallow sandy aquifer. *Geochim. Cosmochim. Acta* 73, 6716–6726. <https://doi.org/10.1016/j.gca.2009.08.026>.